AIAA JOURNAL
Vol. 46, No. 3, March 2008

Technical Notes

TECHNICAL NOTES are short manuscripts describing new developments or important results of a preliminary nature. These Notes should not exceed 2500 words (where a figure or table counts as 200 words). Following informal review by the Editors, they may be published within a few months of the date of receipt. Style requirements are the same as for regular contributions (see inside back cover).

Synthesis and Control of Piezoelectric Resonant Actuation Systems with Buckling-Beam Motion Amplifier

Jun-Sik Kim,* K. W. Wang,† and E. C. Smith‡
Pennsylvania State University,
University Park, Pennsylvania 16802

DOI: 10.2514/1.32216

I. Introduction

PIEZOELECTRIC material-based actuators have shown good potential for various applications, such as trailing-edge flaps for rotary-wing vehicles. These piezoelectric actuators are compact, high force, and high bandwidth devices, but can only provide a limited stroke. This limitation can be critical in cases where large trailing-edge flap deflections or large size rotor blades are needed. Efforts to improve the piezoelectric actuator performance have been carried out by researchers in developing amplification mechanisms of various types [1]. Although the results are promising, it is recognized that actuator authority is still a critical issue for large size rotors.

To advance the state of the art and further enhance the authority of piezoelectric material-based actuation systems, various new ideas have been explored in recent years. A novel motion amplifier has been developed by Jiang and Mockensturm [2,3] to increase the output work transferred through a compliant structure. The concept is to induce elastic and dynamic instability of an axially driven buckling beam to amplify the actuator motion. Through testing on a lab setup, it was concluded that such a concept could result in more compact devices that can dramatically outperform state-of-the-art flap actuators in terms of authority [4]. Such actuators also consist of fewer parts and are lighter than existing designs. Because it is a nonlinear amplifier, how to control such a device is a challenging issue yet to be explored. Another innovative idea to further enhance the authority of piezoelectric actuators is to achieve a high-performance resonant actuation system via mechanical and electrical tailoring [5,6]. From reviewing the current buckling-beam motion amplifier and resonant actuator concepts, it is recognized that an approach that combines the two ideas could further advance the state of the art in achieving high authority, light weight, and compact piezoelectric actuators. In other words, our aim is to seek solutions that can effectively tailor and control the piezoelectric/buckling-beam motion amplifier element to operate as a resonant actuation system. It has been recognized that the nonlinear motion amplification system will encounter the jump phenomena and chaotic motion near the resonant frequency [3]. Therefore, how to effectively control such a resonant actuation system is a challenging issue to be addressed.

The objective of this research is to develop a control law that can effectively use the nonlinear resonant actuation system with buckling-beam dynamics for performance enhancement. In [3], an effective single degree-of-freedom model was derived for system analysis and design. Based on similar approaches presented in [7], an alternative dynamic model is developed in this study for mechanical tailoring and controller design purposes. A feedback linearization control law based on the high-gain estimator concept [8,9] is adopted and modified so that the undesired dynamic responses near the resonant frequency, such as the jump phenomena and chaotic motion, can be avoided.

II. System Description and Model Formulation

An active trailing-edge flap attached on a helicopter rotor blade is illustrated in Fig. 1, where the piezoelectric-stack buckling-beam actuation system is aligned parallel to the blade chord. To achieve the desired trailing-edge flap angle, the actuation system needs to overcome the aerodynamic induced hinge moment [6].

A buckling-beam actuator is illustrated in Fig. 2, where the hinged-clamped beam is attached to a piezoelectric-stack actuator. The beam has an initial geometric imperfection, and it is under the axial static and dynamic loading, which is produced by both the preloading and the piezoelectric-stack actuator at the clamped end.

A. Dynamic Equations of Motion of Buckling-Beam Motion Amplifier

Following a similar approach presented in [7,10], the dynamic equations of motion of the buckling-beam motion amplifier are derived. Assuming that the beam is inextensible, a homogeneous one-dimensional elastic body, neglecting rotary inertia and axial dynamics, and applying the ordering scheme $\hat{w} \approx \mathcal{O}(\varepsilon)$, $\hat{w}^0 \approx \mathcal{O}(\varepsilon^3)$, the dynamic equation of motion of the beam, up to $\mathcal{O}(\varepsilon^3)$, is obtained as

$$m\hat{w}_{,tt} + \hat{c}\hat{w}_{,t} + EI(\hat{w}_{,xxxx}\hat{w}_{,x}^2 + 4\hat{w}_{,xxx}\hat{w}_{,xx}\hat{w}_{,x} + \hat{w}_{,xx}^3 + \hat{w}_{,xxxx}) + \hat{P}\left(\hat{w}_{,xx}^0 + \hat{w}_{,xx} + \frac{3}{2}\hat{w}_{,xx}\hat{w}_{,x}^2\right) = 0 \quad (1)$$

where E is the Young's modulus, I is the moment of inertia of the cross section of the beam, l is the span of the beam, m is the mass per unit length of the beam, and c is the damping coefficient of the beam. Note here that the axial dynamics are neglected because the natural frequency of the axial motion is much higher than that of the transverse motion.

The equation of motion presented in Eq. (1) can be represented by the following terms:

Presented as Paper 2206 at the the 48th AIAA/ASME/ASCE/AHS/ASC Structures, Structural Dynamics & Material Conference, Waikiki, HI, 23–26 April 2007; received 17 May 2007; revision received 14 September 2007; accepted for publication 4 November 2007.

*Postdoctoral Fellow, Vertical Lift Research Center of Excellence; jskim@psu.edu. AIAA Member.

†Difenderfer Chaired Professor in Mechanical Engineering. AIAA Member.

‡Professor of Aerospace Engineering. AIAA Member.

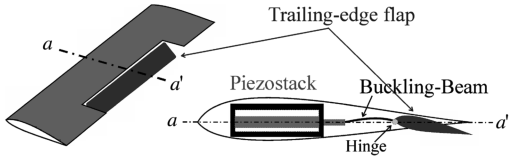

Fig. 1 Actuation system for an active trailing-edge flap.

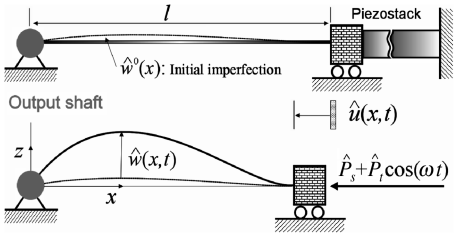

Fig. 2 Schematic of the piezoelectric buckling-beam motion amplifier.

$$w=\frac{\hat{w}}{l},\qquad u=\frac{\hat{u}}{l},\qquad w^0=\frac{\hat{w}^0}{l},\qquad \xi=\frac{x}{l},\qquad \tau=t\sqrt{\frac{EI}{ml^4}}$$
$$\Omega=\omega\sqrt{\frac{ml^4}{EI}},\qquad P=\frac{\hat{P}l^2}{EI},\qquad c=\frac{\hat{c}l^2}{\sqrt{mEI}} \tag{2}$$

and then Eq. (1) can be rewritten as

$$\ddot{w}+c\dot{w}+w''''(w')^2+4w'''w''w'+(w'')^3+w''''+P_s\left\{w^{0\prime\prime}+w''+\frac{3}{2}w''(w')^2\right\}+P_t\left\{w^{0\prime\prime}+w''+\frac{3}{2}w''(w')^2\right\}\cos\Omega\tau=0 \tag{3}$$

B. Nonlinear Dynamics Around the Buckled Configuration

The Galerkin method is adopted to solve the nonlinear buckling equation. The first buckling mode shape ϕ_s of the linear buckling problem for a straight hinged-clamped beam configuration is used to discretize the nonlinear equation given in Eq. (3):

$$w_s(\xi)=b_s\phi_s(\xi),\qquad w^0(\xi)=b_0\phi_s(\xi) \tag{4}$$

where b_s and b_0 indicate the deflections at the middle of the beam span (i.e., at $\xi=0.5$) for buckling and initial imperfection, respectively. The geometric imperfection is assumed to have the same buckling mode shape. This is a reasonable approximation, especially if the magnitude of the imperfection is fairly small.

To obtain the governing equations of beam dynamics around the static equilibrium [7], we let the transverse displacement be

$$w(\xi,\tau)=w_s(\xi)+v(\xi,\tau) \tag{5}$$

where $v(\xi,\tau)$ denotes a time-dependent perturbation around the deformed and/or buckled configuration.

Substituting Eq. (5) into Eq. (3) yields the nonlinear dynamic equation

$$\ddot{v}+c\dot{v}+\mathrm{L}_3(v)+P\mathrm{G}_3(v)+\mathrm{L}_2(v)+P\mathrm{G}_2(v)+\mathrm{L}_1(v)+P\mathrm{G}_1(v)=-P_t\mathrm{G}_0\cos(\Omega\tau) \tag{6}$$

where $P=P_s+P_t\cos(\Omega\tau)$, and $\Lambda_i(v)$ and $\Gamma_i(v)$ are differential operators, which are omitted for the sake of brevity. The preceding equation forms a nonlinear Mathieu–Hill equation with an external excitation.

The nonlinear dynamic equation is discretized via the Galerkin method. A single mode approximation can be then obtained by applying the first mode shape of the linear eigenvalue problem derived from Eq. (6).

$$\ddot{q}+2\mu\Omega_s\dot{q}+(\Omega_s^2+P_tf_1\cos\Omega\tau)q+(\alpha_2+P_tf_2\cos\Omega\tau)q^2+(\alpha_3+P_tf_3\cos\Omega\tau)q^3=-P_tf_e\cos\Omega\tau \tag{7}$$

where Ω_s denotes the first natural frequency, and q represents the first modal magnitude. Expressions for the modal damping ratio $\propto$, parametric excitation magnitude f_i, and external excitation magnitude f_e are not presented here due to space limitations.

III. Output Feedback Linearization Control Using High-Gain Estimator

To obtain the desired output of the beam (the rotation angle at the hinged end $\xi=0$, equivalent to the angular deflection of the trailing-edge flap) at the operating frequency, the piezoelectric-stack actuator needs to be effectively controlled. A feedback linearization control algorithm based on a high-gain estimator [8,9] is developed to achieve such a purpose.

A. State-Space Realization of Nonlinear Dynamic Equation

One can obtain a corresponding state-space form of Eq. (7) as

$$\dot{x}_1=x_2\qquad \dot{x}_2=\Theta(x_1,x_2,\tau)+\beta(x_1)u_C \tag{8}$$

where Θ is the nonlinear function including the damping and forcing terms, u_C is the axial dynamic control load, and β represents the nonlinear geometric shape of the post-buckled beam. In general, the nonlinear function $\Theta(x_1,x_2,\tau)$ has uncertainties due to modeling errors and unknowns. It, therefore, cannot be directly used in the controller design. These uncertainties can be lumped into a new state η and treated as unknown. Then, Eq. (8) becomes

$$\dot{\boldsymbol{X}}=\mathbf{A}\boldsymbol{X}+\boldsymbol{B}(\eta+\beta u_C)\qquad \dot{\eta}=\Xi(x_1,x_2,\eta,u_C,\tau) \tag{9}$$

where

$$\mathbf{A}=\begin{bmatrix}0&1\\0&0\end{bmatrix},\qquad \mathbf{B}=\begin{bmatrix}0\\1\end{bmatrix},\qquad \Xi=\sum_{i=1}^{2}\frac{\partial\Theta}{\partial x_i}\frac{\partial x_i}{\partial\tau}+\frac{\partial\Theta}{\partial\tau} \tag{10}$$

Note that the new function Ξ is also unknown because Θ is unknown.

According to [9], the control law for the tracking problem can designed as follows:

$$u_C=(\dot{x}_{2d}-\eta+\tilde{\mathbf{K}}\boldsymbol{e})/\beta \tag{11}$$

in which the state error vector $\boldsymbol{e}$ and the gain matrix $\tilde{\mathbf{K}}$ can be found in [8,9].

B. High-Gain Estimator

The control law given in Eq. (11) is not realizable because it includes an unknown state η (i.e., the uncertain term Θ). To circumvent this, one can construct an observer to derive estimated state variables using a new state η. Here, a high-gain estimator [8,9] using output measurement x_1 only, is obtained as follows:

$$\begin{aligned}\dot{\tilde{x}}_1&=\tilde{x}_2-\theta E_1(\tilde{x}_1-x_1)\\ \dot{\tilde{x}}_2&=\tilde{\eta}+\tilde{\beta}(x_1)u_C-\theta^2E_2(\tilde{x}_1-x_1)\\ \dot{\tilde{\eta}}&=-\theta^3E_3(\tilde{x}_1-x_1)\end{aligned} \tag{12}$$

where the tilde denotes the estimated value, and E_1, E_2, and E_3 are defined in [9].

The control law for feedback linearization based on the estimated state variables is now read as

$$u_C=(\dot{x}_{2d}-\tilde{\eta}+\tilde{\mathbf{K}}\,\tilde{\boldsymbol{e}})/\tilde{\beta} \tag{13}$$

Here, it is assumed that an estimation of β is available from feedback (i.e., x_1 state variable), so that it can be compensated by the control u_C

even if there are modeling errors in the geometric stiffness terms such as f_1, f_2, f_3, and f_e.

It should be noted here that the large feedback control input to the nonlinear dynamic system can induce the so-called peaking phenomenon, especially when high-gain observers are employed [9]. This would lead to system instabilities. In addition, the current dynamic system includes parametric excitations, and the feedback control input contributes to these excitations via the nonlinear geometric stiffness β. To eliminate these effects, the feedback control law is modified by a saturation function of $\text{sat}(u_C)$, which is defined as follows:

$$u_C^m = \text{sat}(u_C) = \begin{cases} u_C & \text{if } |u_C| \le U_{\max} \\ \text{sgn}(u_C) U_{\max} & \text{if } |u_C| > U_{\max} \end{cases} \tag{14}$$

One of constraints to $U_{\max}$ can be established from Eq. (7), where the well-known Mathieu equation can be obtained by considering linear dynamics and dropping the external forcing term. From [11], the transition curves separating stability from instability can be found.

IV. Numerical Results and Discussion

Numerical results obtained herein are compared with experimental results obtained by Jiang and Mockensturm [2,3], and the performance of the feedback linearization control law is demonstrated via a reference trajectory tracking problem (tracking desired output shaft angle for rotorcraft application). The dimension and material properties of a hinged-clamped beam, which is the same as that used in [3], is presented in Table 1.

A. Linear Vibration Around Buckled Configuration

The natural frequencies of the post-buckled beam are calculated and compared wtih available data reported in [3]. A six-term approximation is used to predict the first four natural frequencies without any imperfections. All four frequencies agree well with those derived via the Elastica theory. Figure 3 shows variations of the first natural frequency for different levels of initial imperfections. Unlike the perfectly straight beam (an ideal beam), the first natural frequency with an initial imperfection starts to decrease as the static end displacement increases, because the corresponding compressive load (to achieve such an end displacement) is significantly lower than the buckling load of an ideal beam. Even for the beam with a fairly small imperfection ($b_0 = 1.83\text{e}-5$), its first natural frequency deviates significantly from the ideal case in the vicinity of $u_s = 0$ because of lower compressive loads.

B. Nonlinear Frequency Response

Nonlinear frequency responses are calculated to further validate the dynamic model. One of them is illustrated in Fig. 4, where the preloading static end displacement u_s is 0.194% (see Fig. 3), the corresponding compressive static load P_s is 19.29 (140.48 N), the driving end displacement $2u_a$ is 0.129%, and the concentrated mass ($m_C = 0.183$ Kg) is attached to the beam at $\xi = 0.05$ to emulate the shaft inertia effect. Note that u_s and u_a values are taken from [3], which corresponds to case A1 in that reference. Because the initial imperfection b_0 is unknown, we adjust its value so that the predicted first natural frequency matches with that measured in the experiment. The final estimated value of b_0 is 0.0012.

Table 1 Parameters used in numerical studies [3]

Parameters	Value
Beam width	12 mm
Beam thickness	0.508 mm
Beam length, l	60 mm
Beam material density	7700 kg/m^3
Beam Young's modulus	200 GPa
System damping	7% critical damping

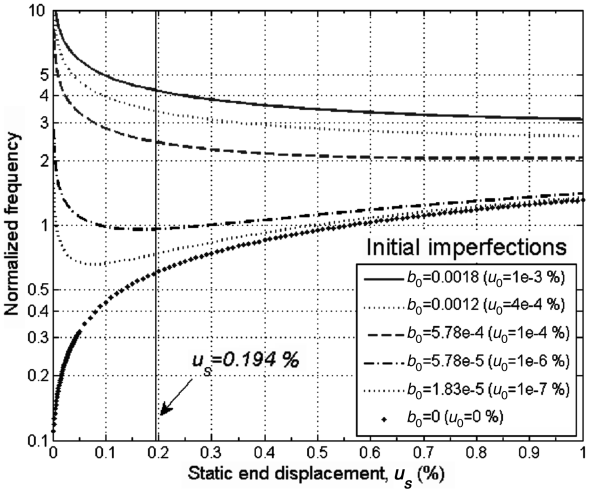

Fig. 3 Variations of the first natural frequency with different initial imperfections.

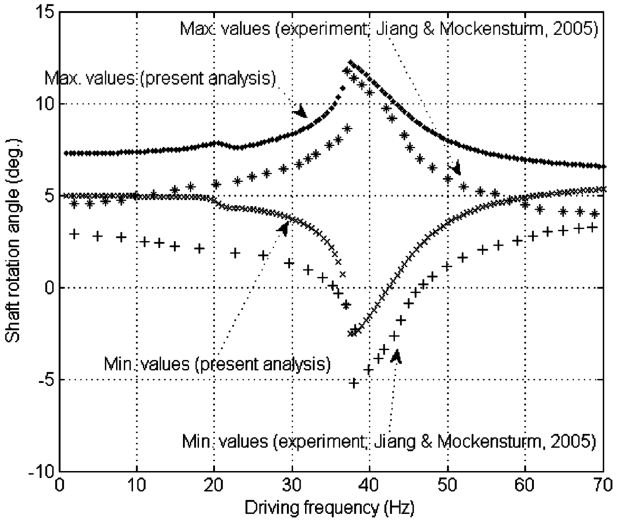

Fig. 4 Comparison of nonlinear frequency responses [2].

As shown in Fig. 4, the simulated results via the "shooting method" match the trend of the experimental results. The present model is able to capture the subharmonic behavior near 20 Hz as well as the softening behavior near the primary resonance (40 Hz). The shaft angle of 14 deg (peak-to-peak) can be achieved near the resonance, in which the driving dynamic load P_t is 0.169 (a corresponding physical value is 1.23 N, which is only 0.884% of the Euler buckling load). This confirms the effectiveness of the buckling-beam motion amplifier.

C. Feedback Linearization Control near Primary Resonance

For the purpose of illustration, a target of ± 4 deg shaft angle with respect to the buckled configuration is assumed for the case study in this paper. This corresponds to an output reference state of $x_{1d}(\tau) = 0.011 \sin(\Omega\tau)$. The control gain is chosen such that $(\mathbf{A} + \mathbf{BK})$ has all its roots located at -1, and the parameters E_1, E_2, and E_3 used in the observer are chosen as one, three, and three, respectively, as recommended in [9]. The parameter θ is set to be five based on parametric study. Here, $U_{\max}$ is set to be one to avoid parametric instability and overshoot response. This corresponds to a physical value of 7.3 N, which is a small value as compared with the Euler buckling load (147 N).

Figure 5 shows the time response of an uncontrolled system and the deviation from the desired shaft angles with frequency sweep down around resonance (from 42 to 35 Hz). Note here that the desired

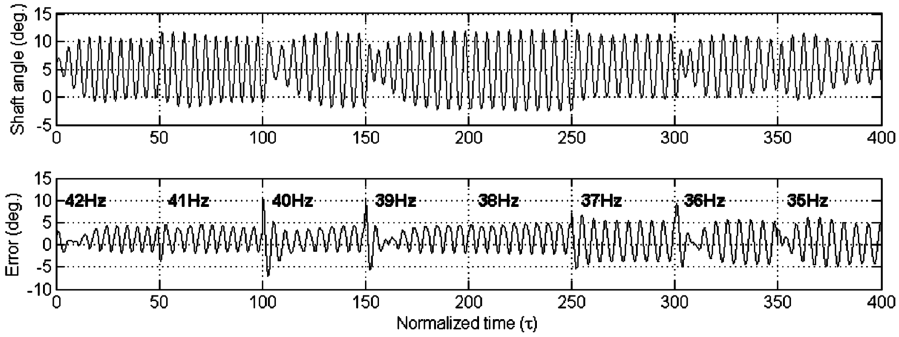

Fig. 5 Time response of uncontrolled system and error with frequency sweep down.

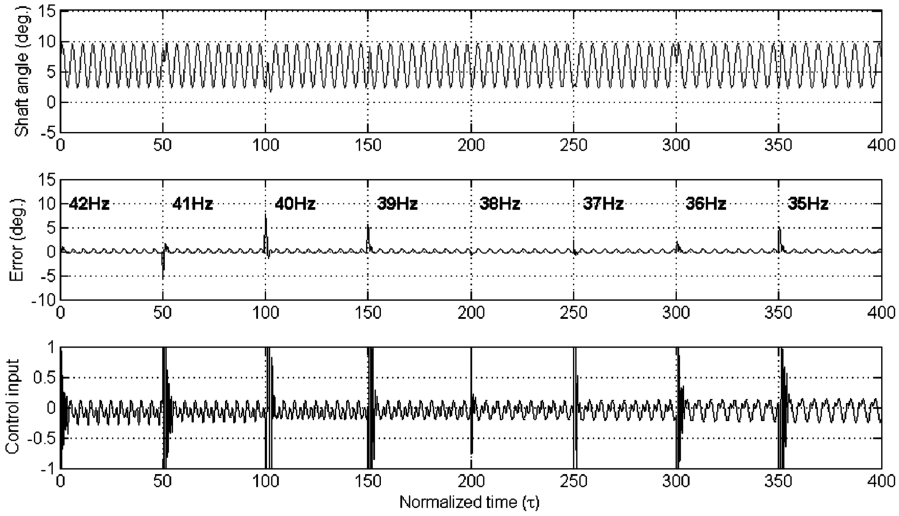

Fig. 6 Time response of controlled system, error, and control input with frequency sweep down.

shaft angles are from 2 to 10 deg, which are ± 4 deg from the static shaft angle (6 deg) induced by the static compressive load P_s. The uncontrolled system shows large deviation from the reference signal in amplitude (up to ± 5 deg) and phase. The observer dynamics agree well with the system dynamics (errors are less than ± 0.5 deg). The time response of a controlled system, the deviation from the desired shaft angles, and the control signal are presented in Fig. 6. One can see that shaft angles of 2 to 10 deg are achieved throughout the time period with very small tracking error. That is, high authority resonant actuation [5] can be accurately controlled by the feedback linearization controller based on a high-gain estimator [9] for the piezoelectric buckling-beam motion amplifier. The quasi-static operation (nonresonant) of the same device with similar level of input is about ± 1 deg. In other words, the proposed approach can achieve a four time increase of authority with good accuracy.

V. Conclusions

In this paper, a nonlinear dynamic model is derived and a robust feedback linearization control law is synthesized to use the high authority feature of a piezoelectric buckling-beam motion amplifier.

Analytical predictions using the nonlinear dynamic model are compared with the experimental results reported in previous literature. Linear vibrations around the buckled configuration are investigated in terms of geometric imperfections and buckling levels. Previous experimental results [2], such as the post-buckling behavior, softening spring effects, subharmonic behavior, and jump phenomena, are captured by the present nonlinear dynamic model.

A high-gain estimator is constructed by treating the nonlinear terms presented in the dynamic model and other modeling errors as bounded uncertainties. The effectiveness of the proposed approach is examined through a case study by tracking the desired shaft angles with frequency sweep down near the resonance (7 Hz bandwidth from 42 to 35 Hz). It is shown that high authority and robust tracking actuation can be achieved. A steady ± 4 deg amplitude is demonstrated, which is four times that which can be achieved (± 1 deg) in a quasi-static (nonresonant) operation with the same piezoelectric buckling-beam actuator.

Acknowledgments

We, the authors, would like to thank Eric Mockensturm at Pennsylvania State University for his invaluable suggestions and for letting us use his and his student's experimental data.

References

[1] Chopra, I., "Status of Application of Smart Structures Technology to Rotorcraft Systems," *Journal of the American Helicopter Society*, Vol. 45, No. 4, Oct. 2000, pp. 228–252.

[2] Jiang, J., and Mockensturm, E., "Motion Amplifier Using an Axially Driven Buckling Beam, 1: Design and Experiments," *Nonlinear Dynamics*, Vol. 43, No. 4, 2006, pp. 391–409. doi:10.1007/s11071-006-0762-x

[3] Jiang, J., and Mockensturm, E., "Motion Amplifier Using an Axially Driven Buckling Beam, 2: Modeling and Analysis," *Nonlinear Dynamics*, Vol. 45, Nos. 1–2, 2006, pp. 1–14. doi:10.1007/s11071-005-0780-0

[4] Szefi, J. T., Mockensturm, E., Smith, E. C., Wang, K. W., Rehrig, P., and Centolanza, L., "Development of a Novel High Authority Piezoelectric Actuator for Rotor Blades with Trailing Edge Flaps," *Proceedings of the 62nd AHS Annual Forum*, Annual Forum Proceedings, American Helicopter Society, Vol. 62, No. 2, May 2006, pp. 840–850.

[5] Kim, J.-S., Wang, K. W., and Smith, E. C., "High Authority Piezoelectric Actuation System Synthesis Through Mechanical Resonance and Electrical Tailoring," *Journal of Intelligent Material Systems and Structures*, Vol. 16, No. 1, 2005, pp. 21–31. doi:10.1177/1045389X05046686

[6] Kim, J.-S., Wang, K. W., and Smith, E. C., "Development of a Resonant Trailing-Edge Flap Actuation System for Helicopter Rotor Vibration Control," *Smart Materials and Structures*, Vol. 16, Dec. 2007, pp. 2275–2285. doi:10.1088/0964-1726/16/6/030

[7] Lacarbonara, W., Nayfeh, A. H., and Kreider, W., "Experimental Validation of Reduction Methods for Weakly Nonlinear Distributed-Parameter Systems: Analysis of a Buckled Beam," *Nonlinear Dynamics*, Vol. 17, No. 2, 1998, pp. 95–117. doi:10.1023/A:1008389810246

[8] Teel, A., and Praly, L., "Tools For Semiglobal Stabilization by Partial State and Output Feedback," *SIAM Journal on Control and Optimization*, Vol. 33, No. 5, 1995, pp. 1443–1488. doi:10.1137/S0363012992241430

[9] Moukam Kakmeni, F. M., Bowong, S., Tchawoua, C., and Kaptouom, E., "Strange Attractors and Chaos Control in a Duffing-Van der Pol Oscillator with Two External Periodic Forces," *Journal of Sound and Vibration*, Vol. 277, Nos. 4–5, 2004, pp. 783–799. doi:10.1016/j.jsv.2003.09.051

[10] Dym, C. L., *Stability Theory and Its Applications to Structural Mechanics*, Noordhoff International, Leyden, The Netherlands, 1974.

[11] Nayfeh, A. H., *Introduction to Perturbation Techniques*, Wiley, New York, 1981.

R. Kapania
Associate Editor